Main Manuscript for

Polyunsaturated fatty acid structure determines the strength of potentiation of Acid-sensing ion channels

Robert C. Klipp[1] and John R. Bankston[1]

[1] Department of Physiology and Biophysics, University of Colorado Anschutz Medical Campus, Aurora, CO, USA.

*Corresponding Author: John Bankston, Department of Physiology and Biophysics, Research Complex 1 North, University of Colorado Anschutz Medical Campus, Aurora, CO, 80045.
Phone: 303-724-4909

E-mail: john.bankston@cuanschutz.edu

Author Contributions: J.R.B. and R.C.K. designed the experiments. R.C.K. performed the experiments. J.R.B. and R.C.K. analyzed the data. J.R.B. and R.C.K. wrote the manuscript.

Keywords: Acid-sensing ion channels, Polyunsaturated Fatty Acids, Arachidonic Acid, Docosahexaenoic Acid

Abstract

Acid-sensing ion channels (ASICs) are sensitized to activation by inflammatory mediators like the polyunsaturated fatty acid (PUFA) arachidonic acid (AA). How lipids like AA potentiate ASICs is not understood. Here we show that fatty acids can cause multiple gating changes in ASIC3 that are consistent with a molecule that stabilizes the open state of the channel. The impact on gating depends on the nature of both the head and tail of the fatty acid with the head group able to dramatically alter the strength of the effect on the channel. N-acyl amino acids (NAAAs) like arachidonoyl glycine (AG) and arachidonoyl serine (AS) are such strong regulators that they can act as ligands at neutral pH. Mutation of an arginine in the outer segment of TM1 (R64) eliminated the PUFA effect. Our results suggest a model where PUFAs bind to ASICs both via their tail group as well as an electrostatic interaction between the charged PUFA head group and the charged arginine side chain. These data provide the first mechanistic look at lipid regulation of ASICs and pave the way for the development of fatty-acid-based therapeutics targeting ASICs.

Main Text

Introduction

Acid-sensing ion channels (ASICs) are voltage-insensitive, pH activated members of the Deg/ENaC family of ion channels[1]. ASICs are widely expressed throughout the body including in neurons in both the central (CNS) and peripheral nervous system (PNS)[1]. They have been demonstrated to impact the sensing of pain and inflammation in the PNS as well as fear conditioning, ischemic cell death, and synaptic plasticity in the CNS[1]. The physiological activation mechanisms of ASICs are not well understood. In pathophysiological conditions like stroke, neurons are exposed to prolonged acidosis[2]. During normal synaptic transmission, it is hypothesized that the synapse becomes transiently acidic after vesicular release of neurotransmitter because the vesicles have a pH ~5[3]. However, this transient, and usually modest, acidification is unlikely to activate many channels in most synapses. There is a growing body of literature suggesting that several endogenous molecules including serotonin, lactate, and nitric oxide act to sensitize ASICs to protons making them more active at less acidic pH[4–7].

The lipid composition of the membrane can significantly impact the function of ion channels. KCNQ1 and GIRK channels require phosphatidylinositol 4,5-bisphosphate (PIP_2) to function while cholesterol can alter the function of nAChR and TRPV1 channels[8–10]. Polyunsaturated fatty acids (PUFAs) have been shown to modulate the large-conductance Ca^{2+}- and voltage-gated K^+ (Slo1 BK) channel with an EC_{50} in the hundreds of nanomolar[11–13]. In addition, the voltage-gated potassium channel, $K_V7.1$, can be either potentiated or inhibited by PUFAs and PUFA-derivatives depending on the structure of the fatty acid[14–20].

Overall, little is known about the role lipids play in ASIC function. Interestingly, a recent structure of full-length ASIC1a from chicken extracted from membranes using SMA copolymer, solved at 2.8Å resolution, revealed multiple ordered elongated

densities consistent with lipids interacting along the transmembrane domains of the channel[21]. Previous structures in detergent micelles adopted substantially different conformations suggesting that lipids are vital to ASIC structure and function[22–24]. Previous work has shown that the PUFA, arachidonic acid (AA), potentiates ASIC function, likely through a direct action on the channel[25,26]. This effect leads to increased pH-activated currents in DRG neurons as well as increased action potential firing in response to modest acidification of the extracellular space around the neuron[25,27]. In addition, exudates, containing lysophophatidylcholine (LPC) and AA, from human patients with inflamed joints could activate ASICs without any change in pH[28]. These early studies suggest that lipids may act as critical sensitizing compounds for this class of channel. However, the mechanism of lipid action on ASICs has been, to this point, unexplored.

Docosahexaenoic acid (DHA) and AA are particularly abundant in the brain and other neuronal tissues[29]. Unesterified PUFAs can result from either synthesis of dietary precursors like linoleic acid, or through liberation from glycerophospholipids via enzymes like phospholipase A2[30]. PUFAs are nutraceuticals with potential to become lead compounds for rational drug design for targeting ion channels and membrane receptors. For instance, PUFAs are being designed as a potential treatment for patients with long QT syndrome type 1[14,17,19,20]. ASICs may present interesting targets for the inhibition of pain and the inhibition of cell death in both ischemia and neurodegenerative disorders[2,31,32].

Here, we examine the structural mechanisms of ASIC regulation by PUFAs and PUFA-derivatives. We show that AA potentiates ASIC3 currents by stabilizing the open state of the channel, impacting several biophysical properties. In addition, by looking at more than 30 different PUFAs and PUFA-derivatives we clearly demonstrate that the ability of PUFAs to act on the channel depend on both the head and tail group of the fatty acid. The properties of the tail group, including length and double bond number, can alter the magnitude of the effect of the PUFA on ASIC3. However, our data show that the head group is likely the critical determinant of fatty acid efficacy in potentiating ASICs. A head group more prone to harboring a negative charge is more likely to act as a strong potentiator of ASIC3 currents. Replacing the carboxyl head group of PUFAs with a negatively charged head group, such as arachidonoyl glycine (AG) and arachidonoyl serine (AS), to form N-acyl amino acids (NAAAs), leads to dramatically larger effects on the channel with each of these compounds capable of acting as a ligand, activating the channel at neutral pH. Finally, we identified a putative interaction site for the PUFA head group on the first transmembrane segment of ASICs near the outer leaflet of the membrane. Taken together, these experiments provide the first look at the structural determinants of lipid regulation of ASICs and could form the basis for pharmacological development of PUFAs or new drugs that target a novel site on ASICs for the treatment of pain or ischemic cell death.

Results

PUFAs stabilize the open state of ASICs.

AA is a highly abundant PUFA with a 20-carbon tail and four cis double bonds. To indicate the length of the tail and the position of the double bonds for the fatty acids

in this manuscript we will use the following nomenclature, [20(5,8,11,14)], which indicates a 20-carbon tail with four cis double bonds at positions 5, 8, 11 and 14. Previous work has shown that ASIC1a and ASIC3 currents elicited by steps to pH 6.9 are increased upon application of 5µM AA to cells expressing these channels[25]. This increase has been shown to be, at least in part, due to an alkaline shift in the pH dependence of activation. We confirmed this initial observation by applying 10µM AA to Chinese Hamster Ovary (CHO) cells expressing ASIC3 with a C-terminal cerulean tag and measured the $pH_{0.5}$ of activation using the whole-cell patch clamp configuration. Coverslips with cells expressing ASIC3 were incubated in 10µM AA for at least 10 minutes and then the currents were elicited via successive steps to more and more acidic pH (Fig. 1A). We found that 10µM AA shifted the $pH_{0.5}$ of activation by 0.11 pH units yet had no effect on the $pH_{0.5}$ of desensitization, in agreement with previous results (Fig. 1B)[27].

Extending these prior observations, we measured the concentration dependence of the shift in the $pH_{0.5}$ of activation. Plotting the shift as a function of AA concentration and fitting to a Hill-type equation (see methods) yielded an EC_{50} of 11.62µM ± 2.08µM (Fig. 1C,1D). This has not been previously measured for ASICs but compares reasonably to values obtained for several other channels that show EC_{50} values can range between 400nm and 100µM[11,17,33]. The maximum shift in the $pH_{0.5}$ of activation measured at any concentration was 0.23 ± 0.02 pH units.

In addition to the shift in activation pH, we observed two previously unreported changes to ASIC3 gating upon AA application. First, there was an increase in the current magnitude upon addition of AA at proton concentrations that should render the channel maximally open (pH 5.5). The amplitude of this current, which we term I_{MAX}, was increased ~1.2 fold upon addition of 10µM AA (Fig. 1E). Surprisingly, there was no additional I_{MAX} increase at 50µM AA despite the increased shift activation $pH_{0.5}$, suggesting the possibility that these effects may arise from distinct mechanisms. Second, at a maximally activating pH of 5.5, a concentration dependent slowing of the rate of desensitization was observed upon addition of AA (Fig. 1F). To quantify this result, we measured the time it takes for the current to decrease 1/e of its original value and found that 50µM AA slowed this time from 427.21ms ± 17.75ms to 739.56ms ± 120.58ms (Fig. 1F). Taken together, these data suggest that AA potentiates ASIC3 by stabilizing the open state of the channel.

Head groups with lower pKa are stronger potentiators of ASIC3 currents.

Structurally, PUFAs contain a negatively charged carboxylic acid head group and a long non-polar acyl tail that can have one to six double bonds in varying positions along the tail. Studies in other ion channels have demonstrated that the PUFA tail length, number, and position of double bonds, as well as the charge and size of the PUFA head group can all contribute to ion channel potentiation[11,16,20,34]. A previous study of PUFA potentiation of ASICs suggested that an increase in the number of double bonds in the PUFA tail increases ASIC potentiation[25]. This hypothesis was based on examination of only four PUFAs and there has been no thorough study examining the other structural components of the PUFA. We therefore sought to determine the important structural elements in PUFA modulation of ASICs.

There are AA-derivatives that vary in their head groups that allowed us to first probe the contribution of the head group in ASIC modulation. We compared AA to eight AA-derivatives with differing head groups and identical tails [20(5,8,11,14)] (Fig. 2A) (Table 1). These head groups vary in size, atomic composition, and propensity to ionize with some that readily ionize (e.g., glycine) and others that do not (e.g., methyl ester).

To compare potentiation among these AA-derivatives, we again measured the pH dependence of activation in the presence of 10µM fatty acid (Table 1). Fatty acids with carboxyl, glycine, serine, or alanine head groups caused significant alkaline shifts in the $pH_{0.5}$ (Fig. 2B). Methyl ester, ethanolamide, methyl amide, and ethyl ester head groups had no significant effect on the pH dependence of activation (Fig. 2B).

In several voltage-gated ion channels a negatively charged head has been crucial for potentiation[11,16,34]. Figure 2C shows the shifts in the activation $pH_{0.5}$ from figure 2B plotted as a function of the calculated pKa of the AA-derivatives. The neutral head groups are shown to left of the scale break on the x-axis at pKa = 7, representing either their lack of ionizable atoms (ethyl ester and methyl ester), or a pKa well outside the range of pH values used in our experiments (ethanolamide and methyl amide). In general, head groups with a lower pKa tended to have a larger potentiation of ASIC3 currents. The reported pKa values were calculated using MarvinSketch and reflect the pKa of the head group connected to the acyl tail in solution, not in a bilayer. Certainly, the local environment of the lipid will have a large impact on the charge of the lipid in a real cell. Regardless, these data suggest that head groups more likely to harbor a negative charge are more effective at potentiating ASIC3.

The two bulkier head groups showed differing effects. Ethanolamide phosphate, which does have a site likely to have a negative charge over the range of pH used here, shifted the $pH_{0.5}$ to a similar degree as the carboxyl head, while the taurine head group, despite its low pKa, had no effect on channel activation (Fig. 2B). This reduced efficacy may stem from steric clashes between these bulkier head groups and the binding site on the channel. Taken together, these data indicate that the charge of the head group can have a profound impact on the ability of the lipid to potentiate ASIC3 currents.

A longer acyl tail is important for PUFA potentiation of ASIC3.

Next, we sought to determine how the structure of the tail impacts regulation of ASICs. PUFA tails are often broken down into four properties: length, number of double bonds, position of the double bonds, and ω-number. To understand how each of these contribute to PUFA modulation of ASICs, we examined a total of 24 PUFAs with identical carboxyl head groups (Table 1). We again measured changes in the pH dependence of activation in response to 10µM PUFA. Figure 3A shows PUFAs with varying tail properties and their respective shifts in the activation $pH_{0.5}$ which ranged from a 0.32 pH unit alkaline shift all the way to a 0.07 acidic shift. These data indicate that the nature of the tail can have a considerable impact on the modulation of the channel.

In determining the tail properties important in PUFA efficacy, we first examined tail length. All PUFAs with an 18-carbon acyl tail had small (< 0.01 pH unit), non-significant, effects, whereas many of the 20- and 22-carbon tail PUFAs shifted ASIC3 $pH_{0.5}$ to a greater extent with several shifting by more than 0.26 pH units (Fig. 3A). This can also be seen in the heat map in figure 3B. Each column of the map represents an

individual tail characteristic of the adjacent PUFA in figure 3A. The magnitude of the shift in activation at 10µM is illustrated by the color scale ranging from dark red (strong alkaline shifts) to dark green (small acidic shift). Although a longer tail length appeared necessary to confer stronger regulation, it was not sufficient. Several PUFAs with 20- and 22-length acyl tails failed to potentiate ASIC3, indicating other tail properties are important to PUFA potentiation.

PUFAs with a longer acyl tail require more double bonds to potentiate ASIC3.

Our data suggest that a minimum of three double bonds in the PUFA tail were necessary for strong potentiation (Fig. 3A, 3B). No PUFAs with either one or two double bonds potentiated ASIC3 currents. Each tail length appears to have an optimal window of required double bonds to effectively potentiate ASIC3. We observed that as the acyl tail got longer, the range of optimal double bonds also increased. For PUFAs with a 20-length tail, strong potentiators all had three to four double bonds. For PUFAs with 22-carbon tails, four to six double bonds were necessary for strong potentiation of ASIC3 (Fig. 3A, 3B).

To look at this more carefully, we measured the shift in $pH_{0.5}$ caused by docosapentaenoic acid (DPA) and nonadecapentaenoic acid (NPA) which share the identical number and position of double bonds but differ in tail length ([22(4,7,10,13,16)] and [19(4,7,10,13,16)], respectively) (Fig. 3C). At 10µM, the 22-carbon tail DPA strongly potentiated ASIC3 ($\Delta pH_{0.5}$ = 0.27), whereas the 19-carbon NPA, had no effect on the channel ($\Delta pH_{0.5}$ = 0.01) (Fig. 3D). These data are consistent with our observations. First, tails of at least 20 carbons are necessary, but not sufficient for strong potentiation. Second, having five double bonds in a longer acyl (22-carbon) tail is compatible with strong modulation, but having the same five double bonds does not result in a good potentiator for shorter tails.

To ensure the differences observed for NPA and other PUFAs that did not alter the activation $pH_{0.5}$ was not an artifact of varying EC_{50} values, we compared the concentration dependent effects for both weak and strong ASIC3 potentiators. To do this we measured the ASIC3 current at the ~$pH_{0.5}$ (6.6) and applied increasing concentrations of PUFA to the same cell (Fig. 3E). The black trace in figure 3E shows fully activated ASIC3 current at pH 5.5. The overlayed traces to the right show currents elicited with a switch to pH 6.6 at increasing concentrations of DPA. These data show that with increasing concentrations of DPA the channel can be maximally activated even at pH 6.6. In contrast, NPA, oleic acid (OA) [18(9)] and dihomo-γ-linolenic acid (DHLA) [20(8,11,14)] which all failed to significantly shift the activation pH in figure 3A also showed no further potentiation of pH 6.6 currents at higher concentrations (Fig. 3F).

A double bond near the head group is important for 22-length PUFAs.

For PUFAs with 18- or 20-length tails, there was no specific double bond position that appeared necessary for potentiation. However, for the 22-length PUFAs, a double bond at position four was present in every strongly potentiating PUFA (Fig. 3A, 3B). DPA [22(7,10,13,16,19)] did not significantly affect ASIC3 while DPA [22(4,7,10,13,16)] with a double bond at position four, had a large (ΔpH = 0.27 pH units) alkaline shift in the activation pH, despite sharing four out of five double bond positions. Likewise,

docosatetraenoic acid [22(7,10,13,16)] failed to alter ASIC3 currents despite having all the same double bonds as DPA [22(4,7,10,13,16)] except for the four-position.

Finally, we examined the relationship between ω-number and the functional effect of the lipid. The ω-number refers to the number of carbons away from the methyl end of the tail that the last double bond appears. Previous work has shown that the ω-number correlates with some effects that PUFAs have on other classes of ion channels[19]. However, there was no relationship between ω-number and the shift in the pH dependence of activation of ASIC3 by PUFAs (Fig. 3B).

Amino acid head groups have larger magnitude effects on ASIC3 currents.

Our data to this point has shown that the structure of the head and tail groups impact the magnitude of the effect that the fatty acid has on ASIC3 function. In principle, this impact can stem from a change in the binding or a change in the ability of the fatty acid to alter ASIC3 function. It is difficult to measure binding directly, but we measured several properties that can be impacted by changes in affinity to see if there were any hints that these structures changed the binding of the lipid for the channel.

First, we compared the EC_{50} of the shift in the pH dependence of activation for AA, DHA, and AG (Fig. 4A). AG and DHA showed a modestly lower EC_{50} values of 5.40µM ± 1.12µM and 4.9µM ± 0.66µM, respectively, compared to 11.62µM ± 2.08µM for AA. However, DHA and AA, both with carboxyl head groups had comparable maximum shifts while AG had a larger maximum shift in the $pH_{0.5}$ (Fig. 4A). Again, while all three of these lipids caused strong shifts in the activation pH, there was little shift in the pH dependence of desensitization (Fig. 4B).

Despite having nearly identical EC_{50} values, the wash on and off kinetics of DHA and AG differed substantially. To test the wash on and off rates, cells expressing ASIC3 were rapidly activated by repeated exposures to a pH of 6.6 followed by a recovery from desensitization at pH 8. Wash on was measured following control measurements by repeating the protocol with 10µM lipid in both solutions. Finally, wash off was measured in the absence of lipid (Fig. 4C). The time course of wash on, as determined by the amount of time to reach 1/e of the maximum effect (see methods), for AG was 5.97s ± 0.73s, approximately six times faster than either AA or DHA, 31.08s ± 4.96s and 29.20s ± 4.98s, respectively (Fig. 4D – 4F). The time to reach 63% wash off for AG, 15.35s ± 0.82s, was two times faster than AA or DHA, 30.18s ± 3.00s and 30.53s ± 1.01s, respectively. However, unlike AA and DHA, AG showed complete wash off while DHA and AA plateaued at values approximately 20% greater than control pH 6.6 values. While none of these results are direct measures of a change in affinity, they are consistent with the idea that the structure of the lipid may alter the binding to the channel which is an expected result.

In addition, we looked at whether the structure of the lipid could alter the efficacy (maximum effect) of the fatty acid. We found that AG was able to act as a ligand for ASIC3, generating a non-desensitizing channel current at neutral (7.4) pH in a concentration dependent manner (Fig. 5A). We measured the magnitude of this current in the presence of DHA, AG, and AS 25s after switching from pH 8 to pH 7.4 and normalized this value to the peak current measured at pH 5.5 in the absence of lipid. On average this resulted in a steady state current that was just under 2% of the peak current in the presence of AG and just over 2.5% of the peak current in AS This effect

appeared to be limited to the NAAAs with lower pKa head groups as DHA did not generate any significant sustained component at pH 7.4 (Fig. 5B).

While the NAAAs were stronger potentiators, the neutral head groups had minimal effects on ASIC3 currents even at high concentrations. To show this, we compared the concentration dependent effects of AA to two weakly potentiating AA-derivatives, methyl ester and ethanolamide, following the same protocol illustrated in figure 3E where we pulse to a single pH (6.6) and add increasing concentrations of PUFA. AA shows a clear concentration dependent increase in pH 6.6 evoked ASIC3 currents while the neutral ethanolamide and methyl ester head groups produce lipids that are weak potentiators of ASIC3 currents even at increasing concentrations of lipid (Fig. 5C).

Given these results, we wondered whether we could convert a poor potentiator into a strong one by only changing the head group to one with a lower pK_a, or conversely reduce the effect of a strong potentiator by replacing the head group with a neutral one. To do this we first compared docosatetraenoic acid [22(4,10,13,16)] with carboxyl head group to a methyl ester head group derivative with the same tail and found that the potentiating effect was significantly reduced with the methyl ester (Fig. 5D). Conversely, both linoleic acid [18(9,12)] and oleic acid [18(9)], which had no statistically significant effect on ASIC3 currents, could both be converted into stronger potentiators upon replacement of their carboxyl head groups with a glycine (Fig. 5D). Although the glycine head group enhanced potentiation of all PUFAs tested, addition of glycine alone (no tail) showed no potentiation, even up to 100µM, illustrating that an acyl tail is required (Fig. 5D). These data show that the head group can convert a fatty acid from a bad potentiator to a good one or vice versa suggesting that the head group is likely the critical determinant of the strength of potentiation.

In addition, the more negatively charged head groups also had a larger impact on the desensitization rate of ASIC3 (Fig. 5E). All potentiating lipids tested also slowed the rate of desensitization in a concentration dependent manner (Fig. 5E,5F). OA, which had no effect on the $pH_{0.5}$, also had no effect on the rate of desensitization. Again, the NAAAs had the largest impact on the rate of desensitization at either 10µM or 50µM. In fact, AS was significantly stronger at slowing desensitization compared to all other PUFAs, including AG.

A more complicated result was seen looking at the changes in I_{MAX} that these fatty acids elicited. These currents were measured by switching between pH 8 and pH 5.5 for 1.5s and then repeating this measure after 120s exposure to the fatty acid (Fig. 5G). Again, at both 10µM and 50µM, application of OA had no effect on I_{MAX}, while all potentiating lipids significantly increased the current at pH 5.5. Surprisingly, unlike the observed effects on the rate of desensitization and the $pH_{0.5}$, the increase in I_{MAX} was the same for all potentiating lipids (~1.2-fold) apart from AS, which was significantly greater than all other lipids, producing an ~2-fold increase in I_{MAX}. (Fig. 5H). Also interesting was that each lipids effect on I_{MAX} was not significantly different at 10µM and 50µM whereas both the slowing of desensitization and shift in activation $pH_{0.5}$ increased going from 10µM to 50µM.

An arginine at the top of TM1 of ASICs is critical for PUFA potentiation.

Given that the charge of the headgroup impacted the strength of lipid potentiation of ASIC3, we hypothesized that there may be residues on the channel near the membrane boundary that are able to make interactions with the charged head groups of the lipid. This has been demonstrated for other channels where interactions occur with Y, R, or K residues[12,16,20,33,35]. We therefore sought to test whether PUFAs modulate ASICs through similar interactions.

We attempted to narrow down the region on the protein important for regulation before making more targeted mutations. First, we examined the sidedness of the PUFA regulation. To do this, we added 10µM AG to the patch pipette and saw no change in current over one minute nor was there any change in the rate of desensitization as compared to control values (Fig. 6A, 6B). Addition of 10µM AG to the extracellular side of the same cell resulted in a rapid increase in both the current as well as a slowing of desensitization (Fig. 6A, 6B). In addition. inclusion of 10µM AG in the patch pipette did not affect the activation $pH_{0.5}$, even after 10 minutes of recording despite steady state being reached within 10s for external application (Fig. 6C, for wash on rates see Fig 4C and 6A).

We next showed that 10µM DHA resulted in an alkaline shift in the pH dependence of activation of ASIC1a (Fig. 6D). This suggests that the site of regulation is likely conserved between these two isoforms. Together these data suggest that PUFAs act on the extracellular leaflet of the plasma membrane and likely require residues conserved between ASIC1a and ASIC3. We found five candidate residues as possible interaction sites (Fig. 6E, 6F). We made 11 channel mutants that would neutralize the potential interaction with the side chain. Not all the mutations produced functional channels (Table 2).

We tested the effect of DHA on these mutants due to its stronger potentiation of ASIC3, rationalizing that we would more easily be able to see reductions in PUFA effects. We found functional mutations in four of the five positions and measured whether 10µM DHA altered the pH dependence of activation in these mutants. A single position, R64Q, eliminated the shift in the activation $pH_{0.5}$ produced by DHA (Fig. 6G). For the Y67C and Y68W mutants, DHA still potentiated the currents, but the effect was reduced compared to WT potentiation. Looking at the structure of ASIC1a from chicken, R64, Y67, and Y431 (R65, Y68, and Y425 in the chicken), are all within 10Å of one another (Fig. 6D). Mutation of the more distal K428, which resides in the β12 strand, to an alanine yielded functional channels that were still fully potentiated by DHA (Fig. 6F). To further confirm that this region of the channel is important for PUFA potentiation of ASICs, we also mutated R64 in ASIC1a. Like with ASIC3, 10µM DHA did not significantly affect the pH dependence of activation of ASIC1a with the R64Q mutation (Fig. 6G). We attempted to mutate position Y431 (in ASIC3) to A and C and Y424 (in ASIC1a) to C and W and these mutant channels either failed to produce currents or rarely produced very small currents (Table 2). In addition, the ASIC3(R64Q) mutation also eliminated DHA's slowing of desensitization (Fig. 6H). Together, these results demonstrate that this region is critical in PUFA's stabilization of ASIC's open state and may serve as the putative PUFA head group binding site.

Discussion

The results of our study provide the first mechanistic insight into lipid regulation of ASICs. We show that interactions between fatty acids and the channel stabilize the open state of the channel which manifests as an alkaline shift in the activation pH, a slowing of the rate of desensitization, and an increase in the current even at saturating pH. In addition, our data show that fatty acids act on the channel via the outer leaflet of the plasma membrane. Critically, we show that while both the tail and head group of the fatty acid help determine the ability of the lipid to potentiate ASIC3 currents, the head group has profound effects on the magnitude of that potentiation. Head groups with lower pKa values tended to have a greater stabilization of the open state of the channel. Finally, we identify critical residues on the extracellular side of TM1 that are necessary for PUFA regulation of ASICs. These residues may represent a binding site for the head group of the lipid or be critical for transferring the effect of lipid binding to the gate.

The acyl tail of the PUFA clearly impacted the ability of the fatty acid to regulate the channel. The presence of a lipid tail was required for potentiation, as glycine with no acyl tail, had no impact on ASIC3 currents. In addition, the length and overall structure of the tail was also important. Shorter 18-length tails showed weak to no potentiation and longer 20- or 22-length tails were necessary, but not sufficient, to confer strong potentiation. Our data suggests that longer tails required more double bonds to potentiate ASIC3 currents. For 22-length PUFAs, a double bond at position four also seemed to be important for strong potentiation of the channel. These data clearly demonstrate that the structure of the tail is critical for the ability of the lipid to alter channel function. More work is needed to understand how the tail structure impacts regulation of ASIC3. The double bonds change the shape and flexibility of the tail and so it is easy to imagine that the more effective PUFAs have tails whose structure more effectively sit in its binding site on the channel[36,37].

Head groups with lower pKa such as the NAAAs arachidonoyl glycine and arachidonoyl serine had the largest effects on stabilizing the open state of ASIC3. Perhaps most strikingly, we were able to convert weakly potentiating PUFAs like linoleic acid [18(9,12)] and oleic acid [18(9)] into significantly stronger potentiators by replacing the carboxyl head group for a glycine. Conversely, we could significantly decrease the ability of docosatetraenoic acid [22(4,10,13,16)] to potentiate ASIC3 current by substituting a methyl ester head group for the normal carboxyl. These data suggest that the head groups have the ability toggle the strength of the potentiation across a multitude of tail structures.

The strongly potentiating NAAAs, like AG and AS, were able to act as a ligand for the channel at neutral pH activating a small but non-desensitizing ASIC3 current. AS in particular also had dramatic effects on both the rate of desensitization and I_{MAX} at pH 5.5. The ability of these NAAAs to act as a ligand likely owes to their ability to create a “window current”. The term “window current” refers to a range of pH values where the channel may activate but not completely desensitize. The alkaline shift in the activation $pH_{0.5}$ without a concomitant impact on the desensitization $pH_{0.5}$ opens a window of pH over which we would predict a non-desensitizing current might arise from application of lipids like AG.

Consistent with the idea that the head group is critical for modulating ASIC currents, mutating R64 eliminated DHA-dependent potentiation of ASIC3 currents. Similarly, mutation of neighboring residues showed a reduction of DHA potentiation,

while a more distal mutation at K428 had no effect. This suggests the possibility that these residues around R64 create a binding surface for the lipid head group on the channel. The presence of a relatively constrained binding site could explain why larger negatively charged PUFAs, like arachidonoyl taurine, failed to potentiate ASIC3 currents. It is important to note that our mutagenesis data are not direct evidence for a binding site but do clearly indicate that this site is important for PUFA modulation of ASICs.

However, we favor the hypothesis that R64 is part of an interaction site for the head group of our lipids. Interaction between a charged head group and residues on transmembrane segments is common for PUFAs regulating other ion channels. For the voltage-gated Slo1 BK channel, the negatively charged head group is thought to make an ion-dipole interaction with a tyrosine in the transmembrane domain of the channel[11,12]. Similarly, $K_v7.1$ regulation by PUFAs is strengthened by head groups with lower pKa[14,16,18,20]. Recent work has suggested that the negatively charged head group interacts with an arginine and a lysine residue on the extracellular side of the voltage sensor and pore domain of $K_v7.1$[38]. In addition, DHA binds to and speeds the desensitization of the pH gated GLIC channel[33]. A crystal structure of the channel in the presence of DHA solved at pH 4, showed the carboxyl head group forming a salt bridge with the guanidinium group of an arginine residue near the extracellular side of a transmembrane helix[33]. We suggest that a similar interaction may be occurring in ASICs. Supporting this idea, two recent structures of ASIC1a from both chicken and human shows endogenous lipid present between TM1 and TM2 of the same subunit immediately adjacent to our putative binding site[21,39].

Interestingly, a recent study looked at mutation of position R64 and showed that the replacement of the arginine with a hydrophobic amino acid led to an alkaline shift in the pH dependence and a slowing of the desensitization[40]. The structures of ASIC1a from chicken shows that this residue undergoes a movement during gating that changes the network of interactions that it makes. It is possible the PUFA head group works by disrupting interactions made by R64 in the closed or desensitized state, or by stabilizing interactions in the open state.

A second hypothesis may be that the PUFA head groups interfere with Ca^{2+} binding to the channel. Ca^{2+} binding to ASIC3 is thought to inhibit the channel and there are several studies that propose the idea that the proton dependence of the channel stems from protons competing off Ca^{2+} ions to unblock the channel as opposed to protons causing a conformational change that opens a gate[41,42]. Interestingly, R64Q is located very close to these putative Ca^{2+} binding residues, E425 and D432, and may even form a salt bridge with E425[22,43]. It is possible that the fatty acids we examine here may be altering the putative Ca^{2+} binding site and thus the gating of the channel.

The physiologically relevant concentration of these fatty acids in the extracellular space or plasma membrane of cells is not well known, however, concentration of unesterified PUFA in plasma has been suggested to be in the 10µM to 50µM range[44–46]. This concentration can increase to as high as 400µM depending on diet and can also increase in many pathological conditions including inflammation, ischemia, and epilepsy[44,46–48]. Earlier studies showed that 10µM AA was sufficient to sensitize skin DRG neurons to firing action potentials during moderate acidosis (pH 7). Our data suggests that higher concentrations of AA may be able to further sensitize these

neurons to firing given that the half-maximal effective concentration was ~11µM. Reports have shown that DHA may represent 8-18% of the fatty acids in the adult brain and make up an astounding 50-70% of the fatty acids found in the rod outer segment in the retina[49,50]. NAAAs like AG have been demonstrated to be important bioactive lipids that regulate ion channels[51].

ASICs have a wide variety of physiological roles in almost every tissue in the body[1]. Our data suggest that ASIC function could vary in different cell types, in part, due to differences in the composition of the plasma membrane. Fatty acid levels can vary substantially in tissue and cell types and may function in tuning the channel proton sensitivity[52]. It is still a matter of debate what pH ASICs are likely to experience at synapses. Work in retinal bipolar cells has shown that the synapse may acidify by 0.2-0.6 pH units[53]. In our experiments, a pH of ~6.6 is required to activate half of the ASIC3 current and a pH of 6.9 would activate almost no ASIC3 currents. However, binding of potentiating lipids shift the activation pH of ASICs to more physiological pH. Therefore the pH range over which ASICs function is likely altered under pathological conditions where PUFA levels are often elevated, like inflammation[30]. Even in the absence of acidification our data suggest that certain lipids can even act as ligands for this family of channels leading them to open in the absence of significant acidification.

Our results here open a number of interesting questions for future work. Could ASICs have multiple binding sites for lipids that are critical for channel function? Our results suggest the possibility that there are two separate sites for PUFAs on the channel. The effect of our fatty acids on $pH_{0.5}$ increases with increasing concentration while the effect on I_{MAX} does not change. This could be because there are separate interactions that control these two biophysical changes. This was recently shown to be the case for the K_v7.1channel[15]. It is also possible the effect on I_{MAX} is the result of an increase in maximum open probability and that this effect is saturated even at 10µM. Future studies looking at single channels in the presence of fatty acids will be needed to fully understand the biophysical changes that occur.

In addition, the lipid lysophophatidyl choline (LPC) was shown to activate ASICs at neutral pH as well[28]. It will be interesting to see if the interaction site is shared between LPC and PUFAs. The lipids are structurally quite distinct as the effective LPCs are LPC(16:0) and LPC(18:1) which have short acyl tails and either zero or one double bond. However, the head group is zwitterionic and contains a negatively charged phosphate group. On the other hand, like fatty acids, LPC acts by shifting the pH dependence of activation to more alkaline pH. Future work using Molecular dynamics will help narrow down the binding interactions between lipids and ASICs.

In summary, we have shown that PUFAs and many of their derivatives can significantly stabilize the open state of ASICs. Fatty acids with head groups with a low pKa, like the NAAAs, are potent activators of ASIC3. These head groups can convert a poorly potentiating fatty acid into a strongly potentiating one. In addition, the NAAAs can activate the channel even at neutral pH. Our data are consistent with a model where the acyl tail interacts with the TM region of ASIC3 while the head group makes an electrostatic interaction with an arginine near the outer leaflet of TM1. This work will provide the framework for future studies looking at modulation of ASICs by other lipids, including LPC. In addition, PUFAs are potential lead compounds for the modulation of ASIC function. Our work identified two potential inhibitors, eicosenoic acid [20(14)] and

eicosadienoic acid [20(11,14)] that will require future investigation. We have thus identified the basic principles for fatty acid modulation of ASIC3 that can form the basis for the design of new compounds to alter ASIC function in neurons.

Materials and Methods

PUFA Nomenclature. For common PUFAs (AA, OA, DHA, etc.) standard abbreviations are used after being defined in the text. Other PUFAs are named using their tail properties in the format of [length(position of double bonds)]. All acyl tail doubles bonds are in the cis configuration for PUFAs and PUFA-derivatives used in this study. Unless otherwise specified, all PUFAs used in this study contain a carboxyl head group. A full list of the PUFAs used in this study with their head groups, tail lengths and position of doubles bonds is given in Table 1.

Materials and Mutagenesis. PUFAs used in this study were purchased through Cayman Chemical. Plasmids for ASIC1a, and ASIC3 each from rat were gifts from David Julius and subcloned into pcDNA3.1. To visualize cell expression, WT, and mutant ASICs a short proline rich linker was used to join mCerulean3 to the C-terminus of the channel. Point mutants used in this study were made using site-directed mutagenesis either in house or through Biozilla services.

Cell Culture and Transfection. Chinese hamster ovary (CHO-K1) cells (ATCC) were cultured in Ham's F12 media with 10% FBS at 37 °C in 5% CO2. Cells at ~70% confluency were transfected with indicated ASIC plasmid DNA. Transfection was achieved either via electroporation with a Lonza 4D Nucleofector unit or through chemical means using Mirus TransIT-Transfection Reagent (Mirus) following the manufacturer's protocols. Following transfection, cells were plated on 12 mm glass coverslips coated in poly-L-lysine.

Electrophysiological Recordings. All experiments were performed in the whole-cell patch-clamp configuration 16–48 h after transfection. Borosilicate glass pipettes (Harvard Apparatus) pulled to a resistance of 2–6 MΩ (P-1000; Sutter Instrument) and filled with an internal solution containing (in mM): 20 EGTA, 10 HEPES, 50 CsCl, 10 NaCl, and 60 CsF, pH 7.2. Extracellular solution contained (in mM): 110 NaCl, 5 KCl, 40 NMDG, 10 MES, 10 HEPES, 5 glucose, 10 Trizma base, 2 CaCl2, and 1 MgCl2, and pH was adjusted as desired with HCl or NaOH. An Axopatch 200B amplifier and pCLAMP 10.6 (Axon Instruments) were used to record whole-cell currents. Recordings were performed at a holding potential of −80 mV with a 5 kHz low-pass filter and sampling at 10 kHz. Rapid perfusion was achieved using a SF-77B Fast-Step perfusion system (Warner Instruments). Fluorescence was visualized on an Olympus IX73 microscope (Olympus) with a CoolLED pE-4000 illumination system (CoolLED).

Experiments in the presence of PUFA were performed under identical conditions as control experiments except solutions contained the indicated concentration of PUFA. pH was measured prior and after addition of PUFA to solution to ensure no pH change occurred. Experiments in the presence of PUFA were all performed with at least a 10min preincubation with PUFA, unless otherwise specified.

To determine the pH dependence of activation we measured a series of sweeps from a holding pH of 8 for 7s followed by a 3s activation pulses at indicated pH. Each activation pH was normalized to the maximally activating pH measured at pH 5.5. For pH dependences using rASIC1a, the same protocol was used except the length of the holding pulse was 50 s and the activation pulse was 700ms to minimize the contribution of tachyphylaxis. Each experiment was measured for 3 sweeps and then averaged.

For pH dependences of desensitization, each sweep was performed using a holding pH of 8 for 5s followed by a 22s application of the desensitization solution at the indicated pH. The amount of desensitization was determined at the end of each sweep by measuring the current elicited by a 1.5s pulse of pH 6.0 solution. Each current measured at pH 6.0 was then normalized to the maximal current produced by pH 6.0 determined from a desensitization pH of 8. Each experiment was measured for 3 sweeps and then averaged.

For paired concentration dependences measured at single pH. Controls were measured using a holding pH of 8.0 applied for 90s, followed by 1.5s application of pH 5.5, followed again by 90s at pH 8.0 and finally 3s application of pH 6.6. Following the control recording, an identical protocol was followed for increasing concentrations of PUFA on the same cell. Currents in the presence of PUFA were divided by the pH 6.6 current for their respective controls before averages were calculated.

To measure the I_{MAX} increases. Cells in the absence of PUFA were exposed to a holding pH of 8 followed by a 1.5s application of pH 5.5. This was followed by incubation with 10µM PUFA achieved by perfusing 10µM PUFA in pH 8 solution for 2min. The activation protocol was then repeated with 10µM PUFA in both pH 8 and pH 5.5 solutions. Following this, incubation, and activation with 50µM PUFA was performed in an identical manner as 10µM. The pH 5.5 current peaks in the presence of PUFA were divided by the pH 5.5 currents in the absence of PUFA to determine the % I_{MAX}. Each experiment was measured for 3 sweeps and then averaged.

To measure desensitization rates. Cells were exposed to a holding pH of 8 followed by 3s application of pH 5.5 either with or without 10µM or 50µM PUFA present. For measurement of the AS desensitization rates pH 5.5 was applied for 6s. Rates were determined as the time to reach 1/e (63%) of the peak of the pH 5.5 current. Each experiment was measured for 3 sweeps and then averaged.

Data and Statistical Analysis. PUFA structures and pKa determinations for the various PUFA head group derivatives were made using MarvinSketch chemical editing software (ChemAxon). Calculations of pKa PUFA molecule (head and tail) in the absence of a bilayer at room temperature. Whole-cell patch clamp current recordings were analyzed using Clampfit 10.6 (Axon Instruments). All data are given as mean ± the standard error of the mean (SEM).

For pH dependences, reported $pH_{0.5}$ values represent the mean of the $pH_{0.5}$ values for each individual experiment as determined by fitting to a hill-type equation in SigmaPlot10.0:

$$I = \frac{1}{1 + 10^{[(pH0.5 - pHx)n]}}$$

Equation 1

where n = hill number and $pH_{0.5}$=half-maximal activating pH.

$$\Delta pH_{0.5} = \frac{\Delta pH_{0.5}max}{[1 + {EC_{50}}/{C}]^n}$$

Equation 2

where n = hill number, EC_{50} = half maximal potentiation, and $\Delta pH_{0.5}$ = shift in the $pH_{0.5}$.

For wash on kinetics, data was normalized setting the control to zero and the maximum current response obtained during wash on to 1. Reported means for the time to reach 1/e (63%) of the maximal response represent the average value for each individual experiment as determined by fitting to an exponential rise to max in SigmaPlot10.0:

$$I = 1 - e^{-\lambda t}$$

Equation 3

where I = fraction of maximal current, λ = rate constant, and t = time.

For wash off kinetics, data was normalized on the same scale as wash on. Therefore, non-zero minimum values reported for wash off represent the fraction of control prior to wash on. Reported means for the time to wash off 1/e (63%) of the maximal response at time 0s represent the average value for each individual experiment as determined by fitting to an exponential decay in SigmaPlot10.0:

$$I = I_0 + e^{-\lambda t}$$

Equation 4

where I = fraction of maximal current, I_0 = minimal current response, λ = rate constant, and t = time.

Statistical testing was performed using the program package R. For statistical testing, p-values are reported in tables as calculated except in cases where p-values were <0.001, where they are reported as such. Figure legends indicate which statistical test was used for each data set. For figures, statistical significance is indicated by the following scale: * $p < 0.05$, ** $p < 0.01$, *** $p < 0.001$. All p-values reported account for multiple comparisons using appropriate test (see below).

For all statistical testing requiring multiple comparisons, a one-way ANOVA was run followed by post-hoc testing. p-values reported in Table 1 represent a Dunnett's post-hoc test performed on all $pH_{0.5}$ data sets in the table compared to the control ASIC3 $pH_{0.5}$ dataset. Statistical testing of PUFA effects on desensitization rates and I_{MAX} were performed in a similar manner comparing control ASIC3 datasets to all other datasets using a post-hoc Dunnett's test. A post-hoc Tukey's test was also used where indicated to compare between groups means of all data sets.

Paired or unpaired student t-tests were performed where indicated for statistical testing between 2 sets of data (e.g., Table 2). All t-tests are two-tailed and unpaired t-tests assume unequal variance.

Acknowledgements

This work was supported by the National Eye Institute R00 EY024267 (to J.R.B.) and the National Institute of General Medical Sciences R35 GM137912 (to J.R.B.) as well as funding from T32 HL007822 (to R.C.K.).

Competing Interest Statement: The authors declare no competing interests.

References

1. Boscardin, E., Alijevic, O., Hummler, E., Frateschi, S. & Kellenberger, S. The function and regulation of acid□sensing ion channels (ASICs) and the epithelial Na+ channel (ENaC): IUPHAR Review 19. *Br J Pharmacol* **173**, 2671–2701 (2016).
2. Dibas, J., Al-Saad, H. & Dibas, A. Basics on the use of acid-sensing ion channels' inhibitors as therapeutics. *Neural Regen Res* **14**, 395–398 (2019).
3. Du, J. *et al.* Protons are a neurotransmitter that regulates synaptic plasticity in the lateral amygdala. *PNAS* **111**, 8961–8966 (2014).
4. Wang, X. *et al.* Serotonin facilitates peripheral pain sensitivity in a manner that depends on the nonproton ligand sensing domain of ASIC3 channel. *J Neurosci* **33**, 4265–4279 (2013).
5. Yu, Y. *et al.* A Nonproton Ligand Sensor in the Acid-Sensing Ion Channel. *Neuron* **68**, 61–72 (2010).
6. Immke, D. C. & McCleskey, E. W. Lactate enhances the acid-sensing Na+ channel on ischemia-sensing neurons. *Nat Neurosci* **4**, 869–870 (2001).
7. Cadiou, H. *et al.* Modulation of acid-sensing ion channel activity by nitric oxide. *J Neurosci* **27**, 13251–13260 (2007).
8. Huang, C. L., Feng, S. & Hilgemann, D. W. Direct activation of inward rectifier potassium channels by PIP2 and its stabilization by Gbetagamma. *Nature* **391**, 803–806 (1998).
9. Loussouarn, G. *et al.* Phosphatidylinositol-4,5-bisphosphate, PIP2, controls KCNQ1/KCNE1 voltage-gated potassium channels: a functional homology between voltage-gated and inward rectifier K+ channels. *EMBO J* **22**, 5412–5421 (2003).
10. Levitan, I., Singh, D. K. & Rosenhouse-Dantsker, A. Cholesterol binding to ion channels. *Front. Physiol.* **5**, (2014).

11. Tian, Y. *et al.* Atomic determinants of BK channel activation by polyunsaturated fatty acids. *Proc Natl Acad Sci U S A* **113**, 13905–13910 (2016).

12. Hoshi, T., Xu, R., Hou, S., Heinemann, S. H. & Tian, Y. A point mutation in the human Slo1 channel that impairs its sensitivity to omega-3 docosahexaenoic acid. *J Gen Physiol* **142**, 507–522 (2013).

13. Hoshi, T., Tian, Y., Xu, R., Heinemann, S. H. & Hou, S. Mechanism of the modulation of BK potassium channel complexes with different auxiliary subunit compositions by the omega-3 fatty acid DHA. *Proc Natl Acad Sci U S A* **110**, 4822–4827 (2013).

14. Bohannon, B. M. *et al.* Polyunsaturated fatty acid analogues differentially affect cardiac NaV, CaV, and KV channels through unique mechanisms. *eLife* **9**, e51453 (2020).

15. Liin, S. I., Yazdi, S., Ramentol, R., Barro-Soria, R. & Larsson, H. P. Mechanisms Underlying the Dual Effect of Polyunsaturated Fatty Acid Analogs on Kv7.1. *Cell Rep* **24**, 2908–2918 (2018).

16. Liin, S. I. *et al.* Polyunsaturated fatty acid analogs act antiarrhythmically on the cardiac IKs channel. *Proc Natl Acad Sci U S A* **112**, 5714–5719 (2015).

17. Bohannon, B. M. *et al.* Polyunsaturated fatty acids produce a range of activators for heterogeneous IKs channel dysfunction. *J Gen Physiol* **152**, e201912396 (2020).

18. Larsson, J. E., Larsson, H. P. & Liin, S. I. KCNE1 tunes the sensitivity of KV7.1 to polyunsaturated fatty acids by moving turret residues close to the binding site. *Elife* **7**, e37257 (2018).

19. Bohannon, B. M., Perez, M. E., Liin, S. I. & Larsson, H. P. ω-6 and ω-9 polyunsaturated fatty acids with double bonds near the carboxyl head have the highest affinity and largest effects on the cardiac IKs potassium channel. *Acta Physiol (Oxf)* **225**, e13186 (2019).

20. Liin, S. I., Larsson, J. E., Barro-Soria, R., Bentzen, B. H. & Larsson, H. P. Fatty acid analogue N-arachidonoyl taurine restores function of IKs channels with diverse long QT mutations. *eLife* **5**, e20272 (2016).
21. Yoder, N. & Gouaux, E. The His-Gly motif of acid-sensing ion channels resides in a reentrant 'loop' implicated in gating and ion selectivity. *eLife* **9**, e56527 (2020).
22. Yoder, N., Yoshioka, C. & Gouaux, E. Gating mechanisms of acid-sensing ion channels. *Nature* **555**, 397–401 (2018).
23. Baconguis, I., Bohlen, C. J., Goehring, A., Julius, D. & Gouaux, E. X-ray structure of acid-sensing ion channel 1-snake toxin complex reveals open state of a Na(+)-selective channel. *Cell* **156**, 717–729 (2014).
24. Jasti, J., Furukawa, H., Gonzales, E. B. & Gouaux, E. Structure of acid-sensing ion channel 1 at 1.9 A resolution and low pH. *Nature* **449**, 316–323 (2007).
25. Smith, E. S., Cadiou, H. & McNaughton, P. A. Arachidonic acid potentiates acid-sensing ion channels in rat sensory neurons by a direct action. *Neuroscience* **145**, 686–698 (2007).
26. Allen, N. J. & Attwell, D. Modulation of ASIC channels in rat cerebellar Purkinje neurons by ischaemia-related signals. *J Physiol* **543**, 521–529 (2002).
27. Deval, E. *et al.* ASIC3, a sensor of acidic and primary inflammatory pain. *EMBO J* **27**, 3047–3055 (2008).
28. Marra, S. *et al.* Non-acidic activation of pain-related Acid-Sensing Ion Channel 3 by lipids. *EMBO J* **35**, 414–428 (2016).
29. O'Brien, J. S. & Sampson, E. L. Fatty acid and fatty aldehyde composition of the major brain lipids in normal human gray matter, white matter, and myelin *. *Journal of Lipid Research* **6**, 545–551 (1965).

30. Wiktorowska-Owczarek, A., Berezińska, M. & Nowak, J. Z. PUFAs: Structures, Metabolism and Functions. *Adv Clin Exp Med* **24**, 931–941 (2015).

31. Diochot, S. *et al.* Black mamba venom peptides target acid-sensing ion channels to abolish pain. *Nature* **490**, 552–555 (2012).

32. Xiong, Z.-G. *et al.* Neuroprotection in Ischemia: Blocking Calcium-Permeable Acid-Sensing Ion Channels. *Cell* **118**, 687–698 (2004).

33. Basak, S., Schmandt, N., Gicheru, Y. & Chakrapani, S. Crystal structure and dynamics of a lipid-induced potential desensitized-state of a pentameric ligand-gated channel. *eLife* https://elifesciences.org/articles/23886 (2017) doi:10.7554/eLife.23886.

34. Börjesson, S. I., Hammarström, S. & Elinder, F. Lipoelectric modification of ion channel voltage gating by polyunsaturated fatty acids. *Biophys J* **95**, 2242–2253 (2008).

35. Börjesson, S. I. & Elinder, F. An electrostatic potassium channel opener targeting the final voltage sensor transition. *Journal of General Physiology* **137**, 563–577 (2011).

36. Sherratt, S. C. R. & Mason, R. P. Eicosapentaenoic acid and docosahexaenoic acid have distinct membrane locations and lipid interactions as determined by X-ray diffraction. *Chem Phys Lipids* **212**, 73–79 (2018).

37. Feller, S. E., Gawrisch, K. & MacKerell, A. D. Polyunsaturated Fatty Acids in Lipid Bilayers: Intrinsic and Environmental Contributions to Their Unique Physical Properties. *J. Am. Chem. Soc.* **124**, 318–326 (2002).

38. Yazdi, S. *et al.* Identification of PUFA interaction sites on the cardiac potassium channel KCNQ1. *Journal of General Physiology* **153**, (2021).

39. Wu, Y., Chen, Z., Sigworth, F. J. & Canessa, C. M. Structure and analysis of nanobody binding to the human ASIC1a ion channel. *eLife* **10**, e67115 (2021).

40. Chen, Z., Kuenze, G., Meiler, J. & Canessa, C. M. An arginine residue in the outer segment of hASIC1a TM1 affects both proton affinity and channel desensitization. *J Gen Physiol* **153**, (2021).

41. Babini, E., Paukert, M., Geisler, H.-S. & Gründer, S. Alternative Splicing and Interaction with Di- and Polyvalent Cations Control the Dynamic Range of Acid-sensing Ion Channel 1 (ASIC1)*. *Journal of Biological Chemistry* **277**, 41597–41603 (2002).

42. Immke, D. C. & McCleskey, E. W. Protons open acid-sensing ion channels by catalyzing relief of Ca2+ blockade. *Neuron* **37**, 75–84 (2003).

43. Paukert, M., Babini, E., Pusch, M. & Gründer, S. Identification of the Ca2+ Blocking Site of Acid-sensing Ion Channel (ASIC) 1. *J Gen Physiol* **124**, 383–394 (2004).

44. Fraser, D. D. *et al.* Elevated polyunsaturated fatty acids in blood serum obtained from children on the ketogenic diet. *Neurology* **60**, 1026–1029 (2003).

45. Elinder, F. & Liin, S. I. Actions and mechanisms of polyunsaturated fatty acids on voltage-gated ion channels. *Front. Physiol.* **8**, (2017).

46. Siddiqui, R. A., Harvey, K. A. & Zaloga, G. P. Modulation of enzymatic activities by n-3 polyunsaturated fatty acids to support cardiovascular health. *J Nutr Biochem* **19**, 417–437 (2008).

47. Kuriki, K. *et al.* Discrepancies in dietary intakes and plasma concentrations of fatty acids according to age among Japanese female dietitians. *Eur J Clin Nutr* **56**, 524–531 (2002).

48. Hammarström, S. *et al.* Increased concentrations of nonesterified arachidonic acid, 12L-hydroxy-5,8,10,14-eicosatetraenoic acid, prostaglandin E2, and prostaglandin F2alpha in epidermis of psoriasis. *PNAS* **72**, 5130–5134 (1975).

49. Skinner, E. R., Watt, C., Besson, J. A. & Best, P. V. Differences in the fatty acid composition of the grey and white matter of different regions of the brains of patients with Alzheimer's disease and control subjects. *Brain* **116 (Pt 3)**, 717–725 (1993).
50. Anderson, R. E. Lipids of ocular tissues: IV. A comparison of the phospholipids from the retina of six mammalian species. *Experimental Eye Research* **10**, 339–344 (1970).
51. Barbara, G. *et al.* T-Type Calcium Channel Inhibition Underlies the Analgesic Effects of the Endogenous Lipoamino Acids. *J. Neurosci.* **29**, 13106–13114 (2009).
52. Calder, P. C. Docosahexaenoic Acid. *Ann Nutr Metab* **69 Suppl 1**, 7–21 (2016).
53. Palmer, M. J., Hull, C., Vigh, J. & von Gersdorff, H. Synaptic Cleft Acidification and Modulation of Short-Term Depression by Exocytosed Protons in Retinal Bipolar Cells. *J. Neurosci.* **23**, 11332–11341 (2003).

Figures and Tables

Table 1: Activation $pH_{0.5}$ values for ASIC3 in the presence of PUFAs and PUFA-derivatives. All values are measured at 10µM external application of lipid unless otherwise indicated. p-values were calculated with post-hoc Dunnett's test the dataset for each row in table comparing each row in table to the Control dataset.

PUFA Tail	PUFA Head	$pH_{0.5}$	SEM	n	p-value
Control		6.56	0.01	70	
18(9)	Carboxyl	6.57	0.04	7	1
18(6,9,12)	Carboxyl	6.59	0.01	11	1
18(6,9,12,15)	Carboxyl	6.62	0.04	6	0.869
18(9,12)	Carboxyl	6.64	0.03	6	0.508
18(9,12,15)	Carboxyl	6.65	0.02	6	0.193
19(4,7,10,13,16)	Carboxyl	6.57	0.02	6	1
20(14)	Carboxyl	6.49	0.02	6	0.424
20(11,14)	Carboxyl	6.49	0.01	4	0.862
20(8,11,14)	Carboxyl	6.60	0.01	5	1
20(5,8,11,14,17)	Carboxyl	6.62	0.02	11	0.618
20(5,8,11,14)	Carboxyl	6.68	0.01	7	0.005
20(5,8,11)	Carboxyl	6.85	0.04	8	< 0.001
20(5,11,14)	Carboxyl	6.85	0.02	4	< 0.001
20(5,8,14)	Carboxyl	6.86	0.04	5	< 0.001
20(11,14,17)	Carboxyl	6.86	0.03	7	< 0.001
20(8,11,14,17)	Carboxyl	6.88	0.03	9	< 0.001
22(13)	Carboxyl	6.54	0.02	6	1
22(7,10,13,16)	Carboxyl	6.55	0.02	6	1
22(13,16,19)	Carboxyl	6.60	0.02	4	1
22(13,16)	Carboxyl	6.58	0.02	6	1
22(7,10,13,16,19)	Carboxyl	6.64	0.03	6	0.369
22(4,10,13,16)	Carboxyl	6.83	0.03	5	< 0.001
22(4,7,10,13,16,19)	Carboxyl	6.83	0.03	5	< 0.001
22(4,7,10,13,16)	Carboxyl	6.84	0.03	4	< 0.001
20(5,8,11,14)	Methyl Amide	6.54	0.05	5	1
20(5,8,11,14)	Ethyl Ester	6.59	0.01	4	1
20(5,8,11,14)	Ethanolamide	6.62	0.04	5	0.912
20(5,8,11,14)	Methyl Ester	6.64	0.03	5	0.648
20(5,8,11,14)	Alanine	6.75	0.02	4	< 0.001
20(5,8,11,14)	Serine	6.86	0.03	7	< 0.001
20(5,8,11,14)	Glycine	6.90	0.03	4	< 0.001
20(5,8,11,14)	Ethanolamide Phosphate	6.67	0.03	6	0.022
20(5,8,11,14)	Taurine	6.52	0.01	4	1
18(9)	Glycine	6.72	0.02	5	< 0.001
18(9,12)	Glycine	6.89	0.02	5	< 0.001
22(4,10,13,16)	Methyl Ester	6.64	0.06	5	0.648
	Glycine (100µM)	6.52	0.01	3	1
Internal AG (0min)		6.58	0.07	3	1
Internal AG (5min)		6.54	0.05	3	1
Internal AG (10min)		6.57	0.04	3	1

Table 2: Activation $pH_{0.5}$ values for ASIC3 and ASIC1a mutants. ASIC3 WT data shown again from Table 1 for comparison. p-values for all other constructs were calculated from unpaired t-tests comparing Control to 10µM DHA datasets.

Construct	Condition	$pH_{0.5}$	SEM	n	p-value
ASIC3 WT	Control	6.56	0.01	70	< 0.001
	10µM DHA	6.83	0.03	5	
ASIC3(R64Q)	Control	6.86	0.03	10	0.593
	10µM DHA	6.85	0.02	7	
ASIC3(Y67C)	Control	6.50	0.04	4	0.025
	10µM DHA	6.64	0.00	4	
ASIC3(Y68W	Control	6.46	0.00	5	< 0.001
	10µM DHA	6.57	0.02	4	
ASIC3(K428A)	Control	6.27	0.02	5	0.017
	10µM DHA	6.57	0.03	4	
ASIC1a WT	Control	6.43	0.05	7	<0.001
	10µM DHA	6.70	0.02	6	
ASIC1a(R64Q)	Control	6.48	0.03	8	0.082
	10µM DHA	6.58	0.04	8	

Non-functional/poorly expressing mutants

Construct	Observable Currents
ASIC3(R64A)	0/7 cells
ASIC3(Y67,68A)	0/8 cells
ASIC3(Y431A)	2/28 cells
ASIC3(Y431C)	1/17 cells
ASIC1a(Y424C)	0/5 cells
ASIC1a(Y424W)	0/7 cells

Fig. 1. AA stabilizes the open state of ASIC3.
(A) Representative whole-cell recordings showing pH dependent activation of ASIC3 ± 10μM AA. (B) pH activation and desensitization curves for ASIC3 ± 10μM AA (Activation $pH_{0.5}$ = 6.68 ± 0.01, n = 7 for AA; and 6.56 ± 0.01, n = 70 for Control. Desensitization $pH_{0.5}$ = 7.00 ± 0.01, n = 6 for AA; and 7.00 ± 0.00, n = 5 for Control). (C) Curves showing the pH dependence of activation of ASIC3 at different concentrations of AA. (D) $\Delta pH_{0.5}$ values from data in C plotted as a function of concentration yields a half-maximal activation concentration (EC_{50}) = 11.62μM ± 2.08μM. (E) (left) Representative pH 5.5-evoked currents from a single cell at different concentrations of AA. (right) Bar plot showing the fractional change in the maximum current measured at pH 5.5 (I_{MAX}) in response to AA (Fold-increase in I_{MAX} = 1.18 ± 0.05, n = 13 for 10μM AA; and 1.27 ± 0.09, n = 10 for 50μM AA). (F) (left) Representative traces and (right) bar plot showing the time to reach 63% decay of peak ASIC3 current at different concentrations of AA measured at pH 5.5 ($t_{63\%}$ = 427.43ms ± 17.75ms, n= 19 for Control; 469.76ms ± 53.48ms, n = 5 for 10μM AA; and 739.56ms ± 120.58ms, n = 5 for 50μM AA). All data given as mean ± SEM. Asterisks in E represent p-values as determined by paired t-tests. Asterisks in F represent p-values as determined by post-hoc Dunnett's test. ** p <0.01 (see methods for details).

Fig. 2. A negatively charged PUFA head group is critical for potentiation of ASIC3.
(A) (top) Structures of AA and (below) head groups used to replace AA's native carboxyl head group, creating the AA-derivatives used in B and C. (B) Activation $\Delta pH_{0.5}$ values for ASIC3 in the presence of 10μM of the indicated AA-derivatives from A (Data given in Table 1). (C) $\Delta pH_{0.5}$ values from B plotted as a function of the of the calculated pK_a for the AA-derivatives. Neutral head groups (light blue) are plotted on a non-numbered scale to the left of the break in x-axis (at pKa = 7) representing that they either are permanently neutral, or the pKa is sufficiently large that head groups remain neutral at all pH values tested. Red asterisk in panels A-C indicates AA with its native carboxyl head group. All data given as mean ± SEM. Asterisks next to bars in B represent p-values as determined by a post-hoc Dunnett's test. Asterisks in B represent p-values as determined by post-hoc Tukey's test. * p < 0.05, ** p <0.01, *** p < 0.001 (see methods for details).**Fig. 3.** Effects of PUFA tail properties on ASIC potentiation.
(A) $\Delta pH_{0.5}$ values for ASIC3 pH dependence of activation induced by 10μM of PUFAs with differing tails. Tails are grouped by tail length and then ordered based on the magnitude of their effect. The exact positions of the tail double bonds are given on the y-axis. (Data in Table 1). (B) Heat map showing various tail properties (length, number of double bonds, and ω-number) for the data in panel A. Each row in panel B corresponds to the PUFA adjacent in panel A. Dark red indicates largest alkaline $\Delta pH_{0.5}$ measured while dark green indicates a small acidic shift. (C) Structures and (D) $\Delta pH_{0.5}$ values for DPA and NPA which identical double bond positions but differing acyl tail lengths and ($pH_{0.5}$ = 6.83 ± 0.03, n = 5 for DPA; and 6.57 ± 0.02, n = 6 for NPA). (E) Representative traces for a single cell showing protocol used to generate data in F. Acidic jumps to pH 5.5 and 6.6 were measured for the control followed by pH 6.6 measurements being made at increasing concentration of DPA. (F) Plot showing the fold increase in current measured at pH 6.6 plotted as a function of PUFA concentration for OA, DHLA, DPA, and NPA. All data given as mean ± SEM. Asterisks in A represent p-values as determined by post-hoc Dunnett's test. Asterisks in D represent p-values as determined by unpaired t-test. * p < 0.05, ** p <0.01, *** p < 0.001 (see methods for details).

Fig. 4. PUFA structure affects apparent affinity for ASIC3.
(A) $\Delta pH_{0.5}$ value plotted as a function of concentration for AA, DHA, and AG (EC_{50} = 11.62μM ± 2.08μM for AA; 4.92μM ± 0.66μM for DHA; and 5.40μM ± 1.12μM for AG.) AA replotted from Fig. 1 for comparison. (B) Plot showing the pH dependence of ASIC3 activation and desensitization in the presence of 10μM AA, DHA, or AG (Activation $pH_{0.5}$ = 6.83 ± 0.03, n = 5 for DHA; and 6.90 ± 0.03, n = 5 for AG. Desensitization $pH_{0.5}$ = 7.07 ± 0.04, n = 6 for DHA; and

7.05 ± 0.01, n = 5 for AG). Control and AA replotted from Fig. 1 for comparison. (C) Representative traces for a single cell showing repeated pH 6.6-evoked currents upon addition and removal of 10µM DHA. (D) Plot showing the wash on kinetics for AA, DHA, and AG. Current normalized by first subtracting the control current from each time point and then dividing by the maximal current response. (E) Plot showing the wash off kinetics for AA, DHA, and AG. Currents at time 0s represents maximal current reached for wash on. Currents measured during AA and DHA wash off were not able to return to control levels (prior to wash on). (F) Bar plot showing time to reach 63% maximal current response (ON) or time to diminish maximal current response by 63% (OFF) as determined by fits (see methods). All data given as mean ± SEM. Asterisks in F represent p-values for between group comparisons as determined by post-hoc Tukey's test. * $p < 0.05$, ** $p < 0.01$, *** $p < 0.001$ (see methods for details).

Fig. 5. Amino acid head groups have the largest effects on the open state of ASIC3.
(A) Representative ASIC3 currents evoked by application of different concentrations of AG at a constant pH of 7.4. (B) Plot showing the sustained current generated at pH 7.4 in the presence of 50µM DHA, AG, or AS ($\%I_{Peak}$ = 0.41 ± 0.19, n = 5 for DHA; 1.86 ± 0.21, n = 7 for AG; and 2.60 ± 0.33, n = 5 for AS). (C) Plot showing the fold increase in current measured at pH 6.6 plotted as a function of lipid concentration for AA and two AA-derivatives with neutral head groups, E and ME. (D) Plot showing the $pH_{0.5}$ values for three PUFAs with carboxyl head groups and their corresponding head group derivatives. Glycine molecule without an acyl tail is also shown. Tail length and double bond position is indicated on the y-axis and head group is indicated in the color key (C=carboxyl, G=glycine, ME=methyl ester). Arrows denote the shift from the carboxyl head group to the substituted head group. Vertical dashed line represents the $pH_{0.5}$ of ASIC3 Control. (E) Representative traces showing the desensitization of ASIC3 currents evoked by an acidic jump to pH 5.5 in the presence of 50µM of various lipids. (F) Plot showing ASIC3 desensitization rates for different lipids at 10µM and 50µM. Rates are given as the time to reach 63% decay of the peak of current measured at pH 5.5. (G) Representative traces showing the change in ASIC3's current magnitude measured at pH 5.5 (I_{MAX}) in the presence of various lipids. Each group of three traces represents a single cell's I_{MAX} prior to lipid application followed by subsequent 2min exposures to 10µM and 50µM lipid. (H) Plot showing the fractional increase in ASIC3 I_{MAX} for various lipids at 10µM and 50µM. All data given as mean ± SEM. Asterisks above bars in B, F, and H represent p-values as determined by post-hoc Dunnett's test. Asterisks for between group comparisons in B, F, and H as determined by post-hoc Tukey's test. Asterisks in D represent p-values as determined by unpaired t-tests. * $p < 0.05$, ** $p < 0.01$, *** $p < 0.001$ (see methods for details).

Fig. 6. PUFA potentiation of ASICs is dependent on an arginine in the outer segment of TM1.
(A) Time course of ASIC3 activations repeated exposure from pH 8 to pH 6.6. Internal application represents 10µM AG within patch pipette, this was followed by activations in the presence of 10µM AG in the external solutions. (B) Plot showing desensitization rates for ASIC3 controls ± 10µM external AG replotted from Fig. 5 and ASIC3 with 10µM internal AG ± 10µM external AG. Internal AG data points are represented as follows: Control is the rate measured 70s after achieving whole cell patch with 10µM internal AG in patch pipette, external AG is the rate measured at 70s after external perfusion of 10µM AG. Rates are given as the time to reach 63% decay of the peak of current measured at pH 5.5. (C) $\Delta pH_{0.5}$ values for ASIC3 activation over time with 10µM AG within the patch pipette. 0 min denotes $pH_{0.5}$ measured immediately after going whole cell compared to control $pH_{0.5}$ values. (D) pH dependence of activation for ASIC1a with and without 10µM DHA ($pH_{0.5}$ = 6.43 ± 0.05, n = 7 for Control; and 6.70 ± 0.02, n = 6 for DHA). (E) Sequence alignment for the extracellular segments of TM1 and TM2 for chicken

ASIC1a, rat ASIC1a, and rat ASIC3. Highlighted residues represent potential PUFA regulation sites. (F) Structure of chicken ASIC1a. Highlighted residues correspond to same colors in C and D. Structure visualized using Chimera 1.12 and PDB 6VTK. (G) Activation $pH_{0.5}$ values for ASIC mutants ± 10µM DHA (Data given in Table 2). (H) (left) Representative traces showing pH 5.5 evoked currents from ASIC3 with R64Q mutation ± 10µM DHA and (right) plot showing ASIC3 WT and ASIC3 with R64Q mutation desensitization rates ± 10µM DHA. Rates are given as the time to reach 63% decay of the peak of current measured at pH 5.5. WT rates replotted from Fig. 5. All data given as mean ± SEM. Asterisks in B for internal AG as determined by paired t-test for internal AG ± 10µM AG. Asterisks in C represent the p-value as determined by Dunnett's test. Asterisks in G represent the p-value as determined by Dunnett's test in Fig. 3 for DHA and unpaired t-tests between ASIC1a ± DHA as well as each mutant ± 10µM DHA. Asterisks in H represent the p-value as determined from Dunnett's test in Fig. 5 for DHA and the p-value determined by an unpaired t-test between R64Q ± DHA. Asterisks in D represent p-values as determined by unpaired t-tests. * $p < 0.05$, ** $p < 0.01$, *** $p < 0.001$ (see methods for details).

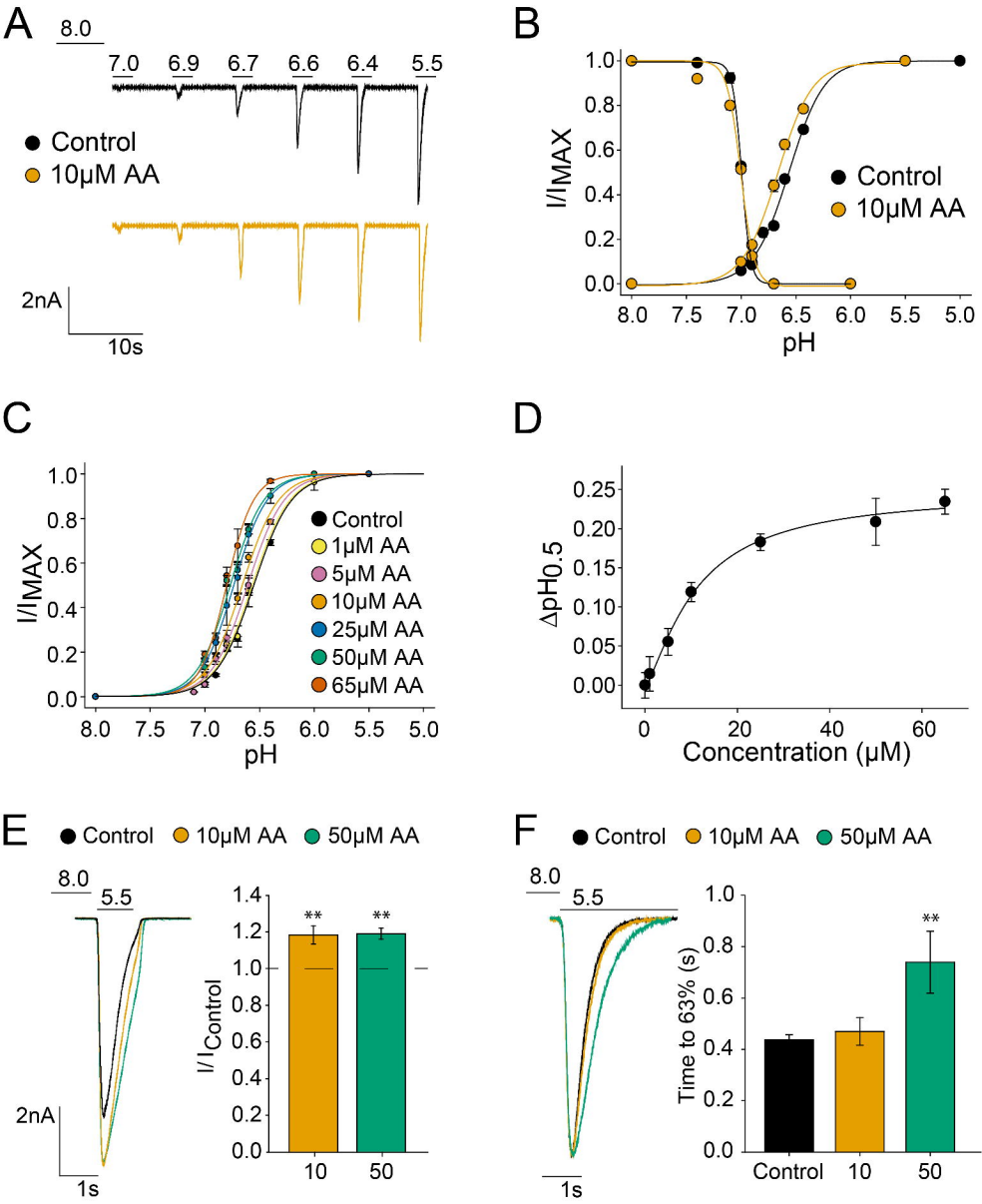
A
8.0
7.0
6.9
6.7
6.6
6.4
5.5
Control
10μM AA
2nA
10s
B
I/IMAX
pH
Control
10μM AA
C
I/IMAX
pH
Control
1μM AA
5μM AA
10μM AA
25μM AA
50μM AA
65μM AA
D
ΔpH0.5
Concentration (μM)
E
Control
10μM AA
50μM AA
8.0
5.5
2nA
1s
I/ IControl
10
50
F
Control
10μM AA
50μM AA
8.0
5.5
1s
Time to 63% (s)
Control
10
50

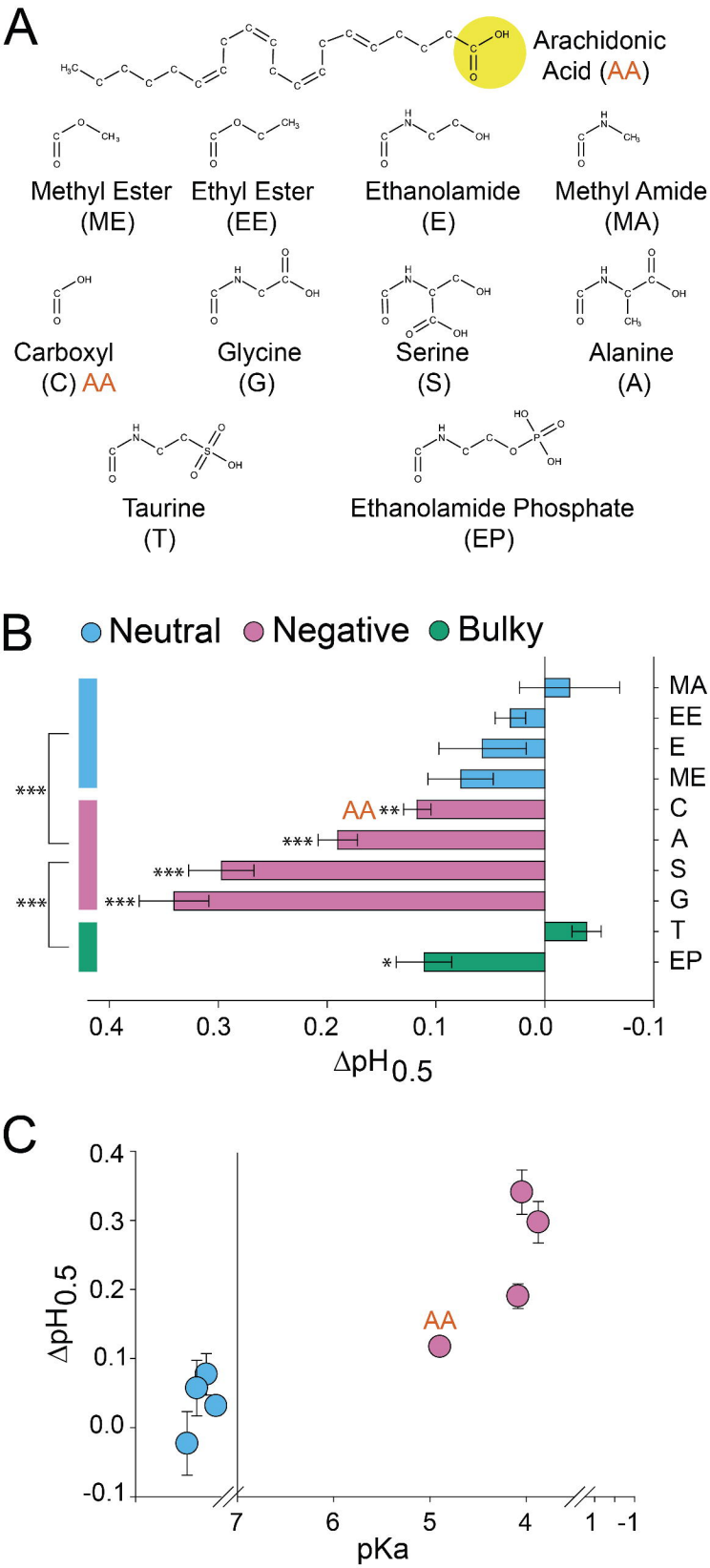
A
Arachidonic Acid (AA)
Methyl Ester (ME)
Ethyl Ester (EE)
Ethanolamide (E)
Methyl Amide (MA)
Carboxyl (C) AA
Glycine (G)
Serine (S)
Alanine (A)
Taurine (T)
Ethanolamide Phosphate (EP)
B
Neutral
Negative
Bulky
MA
EE
E
ME
C
A
S
G
T
EP
AA
***
**
*
0.4
0.3
0.2
0.1
0.0
-0.1
ΔpH0.5
C
AA
ΔpH0.5
pKa
7
6
5
4
1
-1

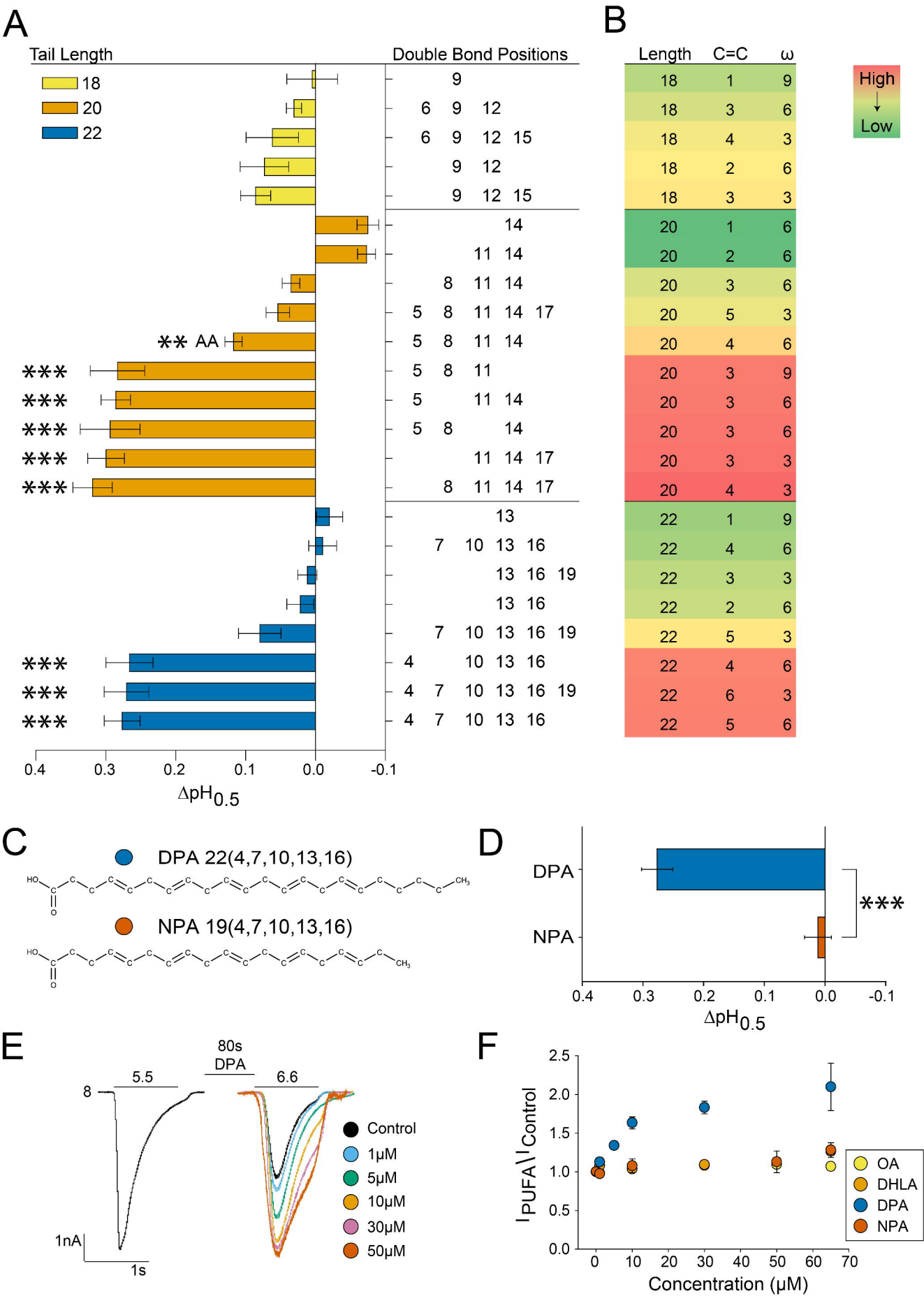
A
Tail Length
Double Bond Positions
18
20
22
** AA
***
0.4
0.3
0.2
0.1
0.0
-0.1
ΔpH0.5
B
Length
C=C
ω
High
Low
C
DPA 22(4,7,10,13,16)
NPA 19(4,7,10,13,16)
D
DPA
NPA
***
ΔpH0.5
E
80s
DPA
5.5
6.6
8
1nA
1s
Control
1μM
5μM
10μM
30μM
50μM
F
IPUFA\IControl
Concentration (μM)
OA
DHLA
DPA
NPA

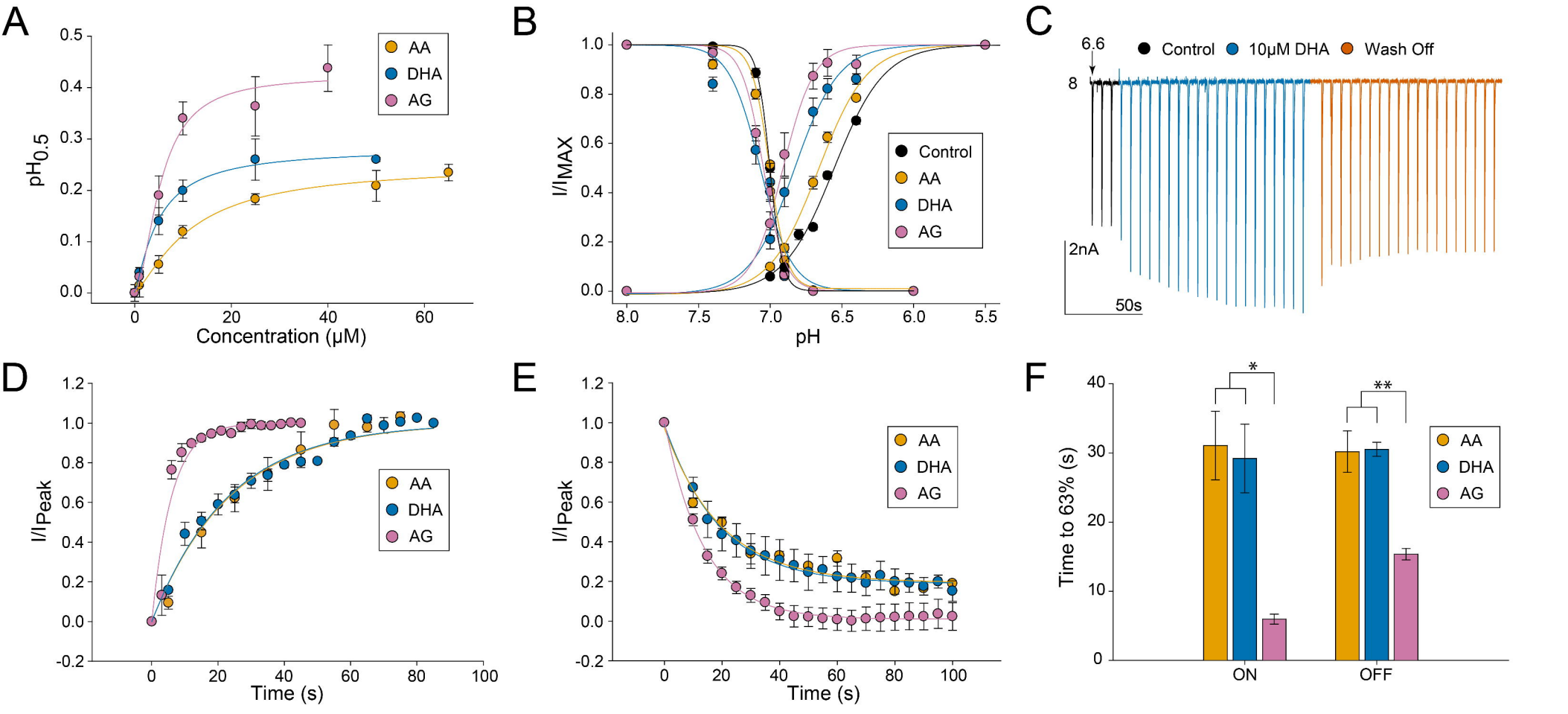
A
pH0.5
Concentration (μM)
AA
DHA
AG
B
I/IMAX
pH
Control
AA
DHA
AG
C
6.6
8
Control
10μM DHA
Wash Off
2nA
50s
D
I/IPeak
Time (s)
AA
DHA
AG
E
I/IPeak
Time (s)
AA
DHA
AG
F
Time to 63% (s)
*
**
ON
OFF
AA
DHA
AG

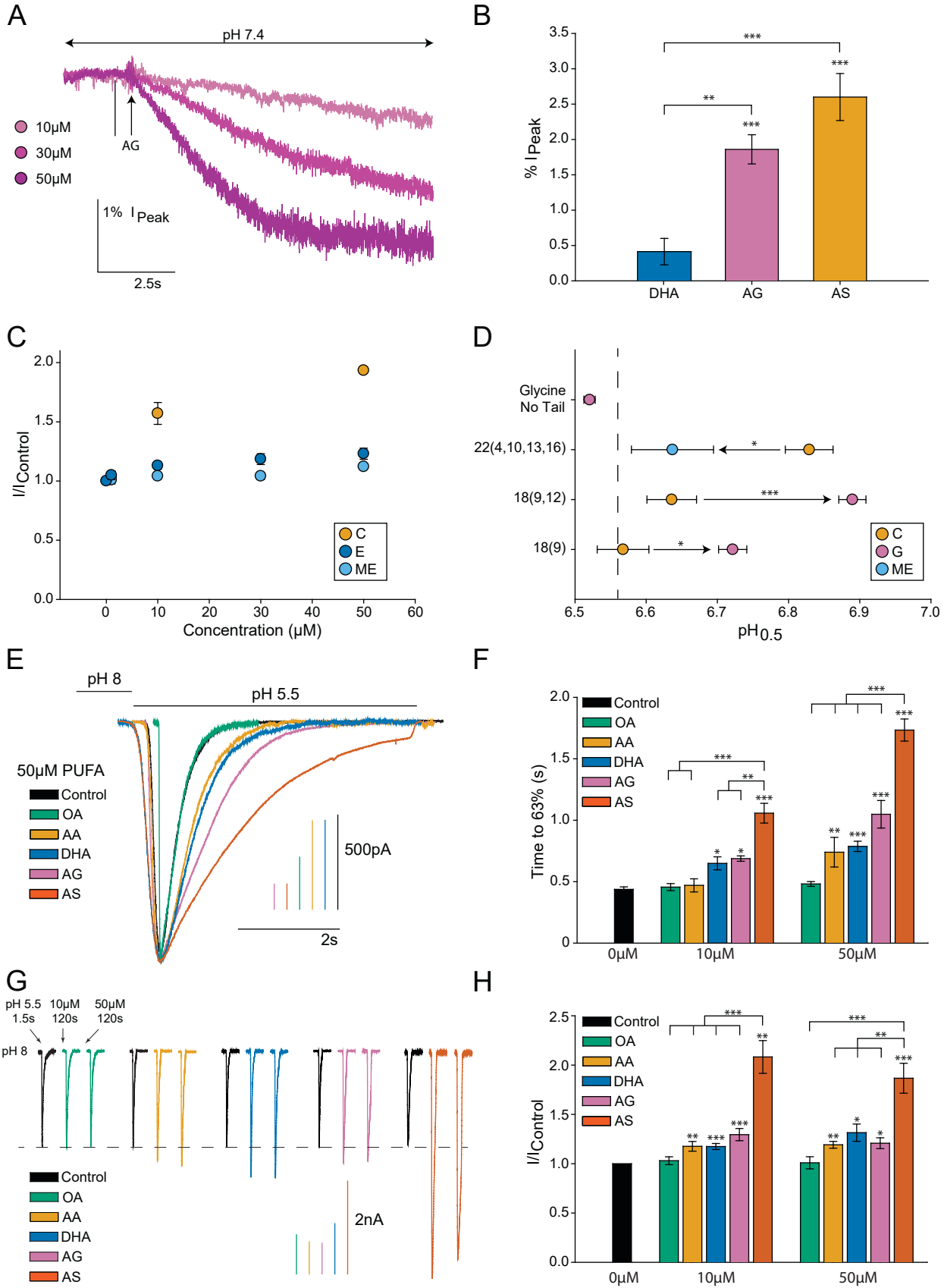
A
pH 7.4
10μM
30μM
50μM
AG
1% I Peak
2.5s
B
% I Peak
DHA
AG
AS
C
I/I Control
Concentration (μM)
C
E
ME
D
Glycine
No Tail
22(4,10,13,16)
18(9,12)
18(9)
pH 0.5
C
G
ME
E
pH 8
pH 5.5
50μM PUFA
Control
OA
AA
DHA
AG
AS
500pA
2s
F
Time to 63% (s)
0μM
10μM
50μM
G
pH 5.5
1.5s
10μM
120s
50μM
120s
pH 8
2nA
H
I/I Control

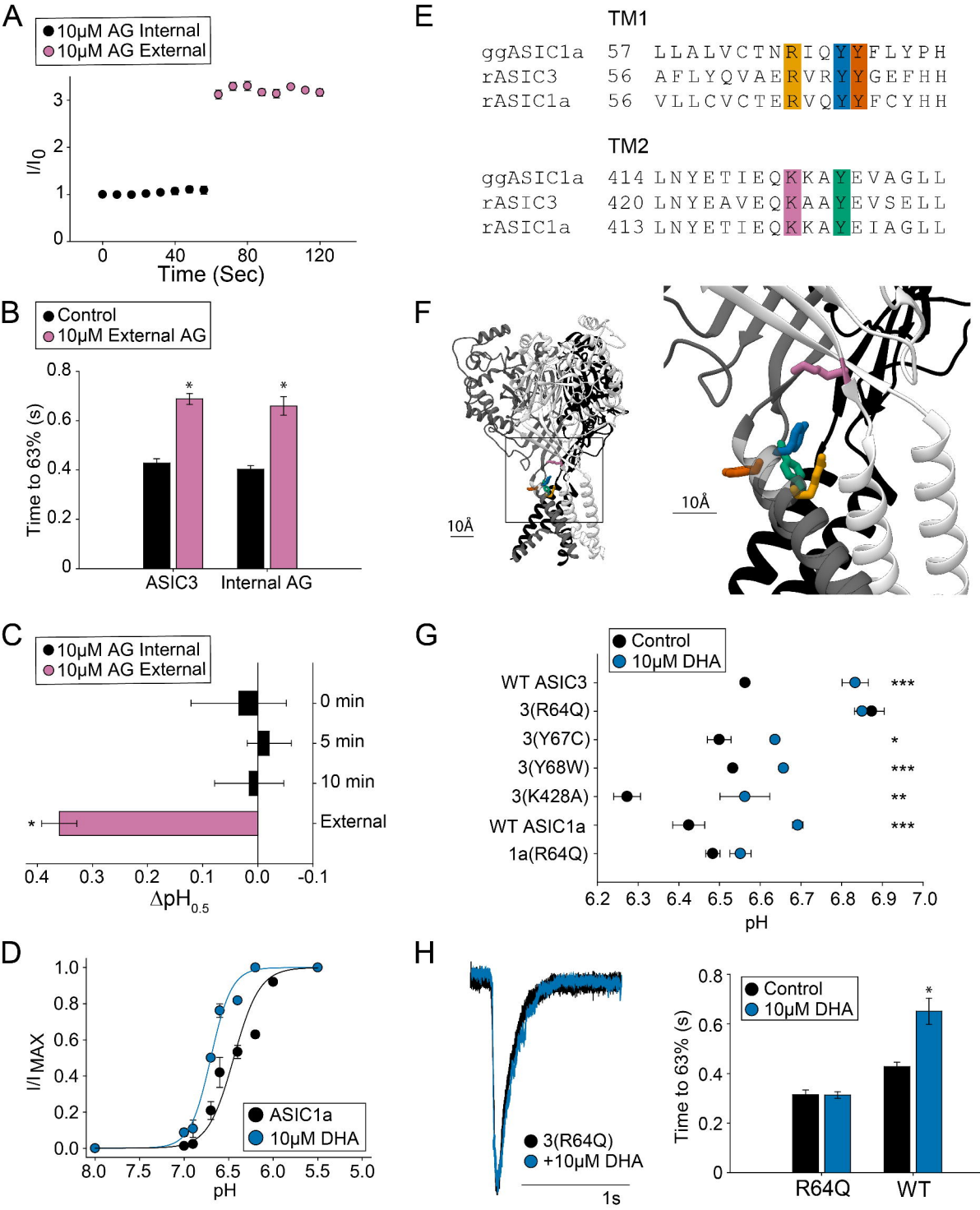
A
10μM AG Internal
10μM AG External
I/I0
Time (Sec)
B
Control
10μM External AG
Time to 63% (s)
ASIC3
Internal AG
C
10μM AG Internal
10μM AG External
0 min
5 min
10 min
External
ΔpH0.5
D
I/IMAX
pH
ASIC1a
10μM DHA
E
TM1
ggASIC1a 57 LLALVCTNRIQYYFLYPH
rASIC3 56 AFLYQVAERVRYYGEFHH
rASIC1a 56 VLLCVCTERVQYYFCYHH
TM2
ggASIC1a 414 LNYETIEQKKAYEVAGLL
rASIC3 420 LNYEAVEQKAAYEVSELL
rASIC1a 413 LNYETIEQKKAYEIAGLL
F
10Å
10Å
G
Control
10μM DHA
WT ASIC3
3(R64Q)
3(Y67C)
3(Y68W)
3(K428A)
WT ASIC1a
1a(R64Q)
pH
H
3(R64Q)
+10μM DHA
1s
Control
10μM DHA
Time to 63% (s)
R64Q
WT